第 34 卷第 7 期
2018 年 7 月

无 机 化 学 学 报
CHINESE JOURNAL OF INORGANIC CHEMISTRY

Vol.34 No.7
1373-1380

烧结反应对液相法制得 $FeWO_4$ 微米晶光催化性能的改性

杜泉岭　后　浩　叶同奇　周红洋*

(合肥工业大学宣城校区化工与食品加工系,宣城　242000)

摘要: 通过简单的液相法制得 $FeWO_4$ 微米晶,$FeWO_4$ 微米晶于 310 ℃、空气气氛条件下烧结,研究了烧结反应对 $FeWO_4$ 微米晶光催化性质的影响。烧结前后的样品通过 X 射线粉末衍射、扫描电子显微镜、透射电子显微镜、N_2 吸附-脱附、热重分析、红外分析和紫外-可见等分析方法加以表征。光催化实验证明烧结后其在降解罗丹明 B 溶液中表现出了较高活性,说明烧结反应有利于提高 $FeWO_4$ 的吸附与光催化性能。

关键词: $FeWO_4$; 烧结; 光催化

中图分类号: O643.36　　**文献标识码**: A　　**文章编号**: 1001-4861(2018)07-1373-08

DOI:10.11862/CJIC.2018.182

Effects of Annealing on Photocatalytic Properties of $FeWO_4$ Microcrystals via Solution-Based Synthesis Method

DU Quan-Ling　HOU Hao　YE Tong-Qi　ZHOU Hong-Yang*

(*Department of Chemical Engineering and Food Processing, Hefei University of Technology Xuancheng Campus, Xuancheng, Anhui* 242000, *China*)

Abstract: $FeWO_4$ microcrystals were fabricated through a simple solution-based route. Then, $FeWO_4$ samples were annealed under the circumstance of air, with the temperature of 310 ℃, and the annealing process is firstly studied for its influence on $FeWO_4$ microcrystals. The $FeWO_4$ microcrystals, before and after annealing treatment, were characterized by XRD, SEM, TEM, N_2 adsorption-desorption, TG, IR, and UV-Vis analysis. Annealed $FeWO_4$ samples show highly active in degradation of rhodamine B (RhB). It reveals that the adsorptive and photocatalytic properties of $FeWO_4$ microcrystals are probably enhanced through annealing treatment.

Keywords: $FeWO_4$; annealing; photo-catalysis

0 Introduction

The expansion of a wide range of chemical contaminants both in air and water is becoming a critical worldwide issue. Photocatalysis, especially photocatalysis employing semiconductor nanomaterials, appears to be the very appealing route than the conventional chemical oxidation methods for decomposition of toxic compounds to non-hazardous product[1]. Fe-based nanomaterials, including iron oxides, $FeVO_4$, $Fe_2(MoO_4)_3$, $FeWO_4$, $FeIn_2S_4$, Fe_3O_4-TiO_2, Fe-CuS-RGO are investigated for their photocatalytic property with these advantages: cheap, non-toxic, environmental friendly, abundant in reserves, broad absorption spectral, and so on[2-5].

The fabrication of self-assembled hierarchical microstructures of inorganic materials with hierarchy architectures and well-defined properties is of great

收稿日期:2018-03-02。收修改稿日期:2018-04-26。

安徽省自然科学基金(No.1508085QB46)资助项目。

*通信联系人。E-mail:zhy2003@hfut.edu.cn

interest to material scientists over the past decades[6]. Iron tungstate ($FeWO_4$), along with the name of "ferberite", is an isostructural compound that crystallizes in a wolframite-type monoclinic structure belonging to the *P2/c* space group[7]. $FeWO_4$ nanomaterials, with various morphologies, were fabricated for its photocatalytic, magnetism, and electrochemical property[7a,8], *etc*. Yu studied the effect of the volume ratios of H_2O and EG solvent on the morphology of $FeWO_4$. In particular, the photocatalytic property was studied to explore their potential application[9]. Monodisperse spindle-like $FeWO_4$ microcrystals were synthesized, which show high active for the photodegradation of methyl orange[10]. Ionic liquid was introduced in reaction system for the synthesis of $FeWO_4$ microspheres[11]. Network-like ZnO-$FeWO_4$ mesoporous heterojunctions with tunable band gaps were prepared for their enhanced visible light photocatalytic performance[12a].

Herein, a solution-based route was introduced to the fabrication of $FeWO_4$ microcrystals, and Na_2EDTA was employed as complexing agent, CTAB was employed as surfactant in the reacting system; the annealing treatment was studied for its influence on $FeWO_4$ microcrystals′ photocatalytic activity, and the temperature of 310 ℃ was carefully chosen. As shown in the following parts, after the annealing treatment, the crystallinity and surface composition of $FeWO_4$ microcrystals were changed. The $FeWO_4$ microcrystals were investigated in the degradation of organic contaminants, and rhodamine B (RhB) was employed as model reagent.

1 Experimental

1.1 Synthesis of $FeWO_4$ Microcrystals

$FeWO_4$ microcrystals were synthesized via a solution-based and route. A typical experiment for synthesizing $FeWO_4$ was as follows: Firstly, with magnetic stirring, 2.0 mmol·L^{-1} $FeSO_4·7H_2O$ and Na_2WO_4 were dissolved into two 50 mL beakers, which included 15 mL distilled water. Then, 1.0 mmol·L^{-1} Na_2EDTA was added into the $FeSO_4$ solution, and dissolved completely. The Na_2WO_4 solution was added to the above mixed solution. Finally, 0.1 g CTAB was added and dissolved. By employing 1.0 mol·L^{-1} NaOH solution and 1 mol·L^{-1} HNO_3 solution, the pH value was adjusted to 8.0. The solution was transferred into a 50 mL Teflon-lined stainless steel autoclave and maintained in an oven at 180 ℃ for 12 h. As the autoclave cooled down naturally to room temperature, the product was collected and washed with distilled water and absolute ethanol at least three times to remove impurities, and was then dried at 80 ℃ for 6 h. At last, the product was annealed under the circumstance of air in the muffle furnace, and the temperature was set at 310 ℃.

1.2 Characterization

The obtained $FeWO_4$ samples were characterized on a Philips X′Pert Pro Super X-ray powder diffractometer with Cu $K\alpha$ radiation (λ=0.154 187 4 nm), the working voltage was set to 40 kV, and the working current was set to 30 mA, and the scanning area was from 10° to 80°. The morphology was examined with a JEOL JSM-6490F scanning electron microscope (SEM), a Hitachi (Tokyo, Japan) H-800 TEM at an accelerating voltage of 200 kV, and a high-resolution transmission electron microscope (HRTEM) (JEOL-2010) operated at an acceleration voltage of 200 kV. Energy dispersive spectrometer (EDS) analysis was obtained with an EDAX detector installed on the same SEM. The X-ray photoelectron spectra (XPS) were collected on a Thermo Scientific ESCALAB 250Xi X-ray photoelectron spectrometer. FT-IR spectra were recorded on a Nicolet Model 759 Fourier Transmission Infrared spectrometer with wavenumbers in the range of 500~4 000 cm^{-1}. Brunauer-Emmett-Teller (BET) specific surface area was determined from nitrogen adsorption at 77 K on a Tristar Ⅱ 3020 M surface area and pore size analyzer. The optical properties of $FeWO_4$ samples were studied by UV-Vis diffuse reflectance spectra on a Lambda 950 spectrophotometer. Thermogravimetric analysis (TGA) was carried out on a TGA-50 thermal analyzer (Shimadzu Corporation) at a heating rate of 10 ℃·min^{-1} in air.

1.3 Photocatalytic test

The photocatalytic activities of the $FeWO_4$

microcrystals before and after annealing treatment were evaluated through the degradation experiment of RhB in an aqueous solution under UV and visible light from a 500 W Xe lamp (modeling sunlight). 30 mg $FeWO_4$ microcrystals photocatalyst was poured in 30 mL of RhB aqueous solution (with the concentration of 30 $\mu mol \cdot L^{-1}$) at room temperature. Before light was turned on, the solution was continuously stirred for 30 min in the dark to ensure the establishment of an adsorption-desorption equilibrium. The concentration of RhB during the degradation was monitored by colorimetry using a SolidSpec-3700 spectrophotometer at room temperature.

2 Results and discussion

2.1 Phase and morphology analysis of $FeWO_4$ before and after the annealing process

The crystallite and phase of as-prepared $FeWO_4$ samples were characterized by X-ray powder diffraction patterns. The diffraction patterns of $FeWO_4$ powders are shown in Fig.1(a) (unannealed line). Comparing with the standard card (PDF No.85-1354), the product could be indexed as a monoclinic-phase of $FeWO_4$ (space group of $P2/c$), with the calculated lattice constants of a=0.472 nm, b=0.57 nm, c=0.495 4 nm, and β=90°. No other peaks were detected, indicating

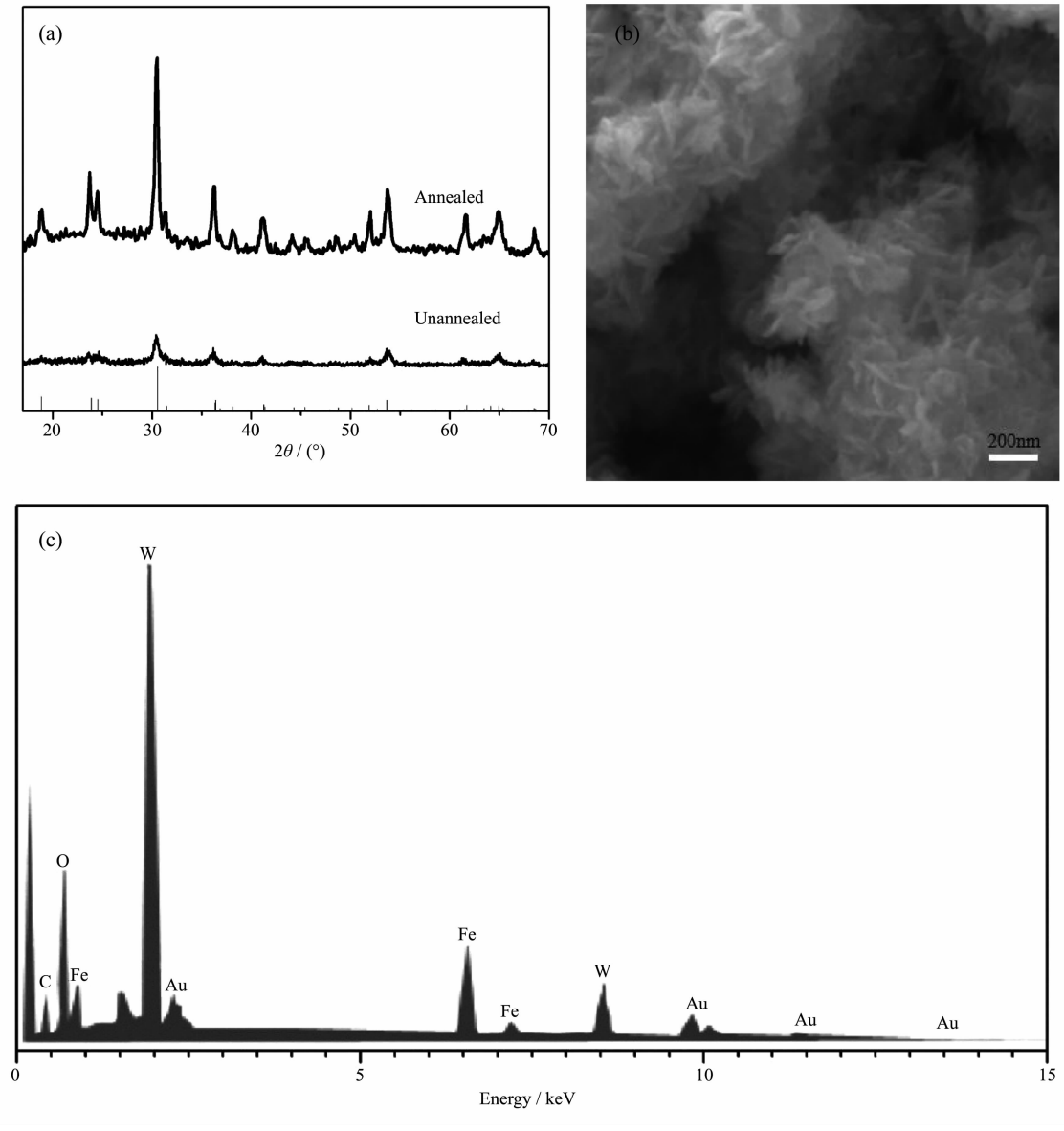

Fig.1 (a) XRD patterns of $FeWO_4$ samples; (b) SEM images of crossed $FeWO_4$ nanoflakes; (c) EDS spectrum of $FeWO_4$ nanoflakes

the purity of the sample. As shown in the SEM images of Fig.1(b), $FeWO_4$ microcrystal is composed of crossed nanoflakes; and the width of these nanoflakes are from 50 to 200 nm. The element and composition of the products were studied via EDS analysis in Fig.1 (c), labeled to be the peaks of Fe, W and O elements in the EDS spectrum. Peaks of Au element are originated from the Au grid. The peaks of C element probably result from organic residue. The TEM image of $FeWO_4$ microcrystal is shown in Fig.2(a), and the HR-TEM image (Fig.2(b)) taken from a part of a typical $FeWO_4$ nanoflake, displays the clearly resolved lattice fringes, indicating the integrality of crystallinity. The inter-planar spacing was measured as 0.295 and 0.38 nm, corresponding to the $(\bar{1}11)$ and (110) plane of $FeWO_4$ monoclinic-phase respectively, with the angle of 98.8°, which is consistent with the literature result[12b].

XRD patterns of annealed and unannealed $FeWO_4$ powders are provided for comparing. As shown in Fig.1(a), all of the peaks are labeled to pure $FeWO_4$ monoclinic-single crystals, in good agreement with the literature results (PDF No.85-1354), no any impurity formed during the annealing process. The result indicated that the crystallinity of $FeWO_4$ nanoflakes is improved during the annealing treatment. Furthermore, the SEM images in Fig.3 indicated that the $FeWO_4$ nanoflakes morphology unchanged during the annealing treatment, with only a little of cracking.

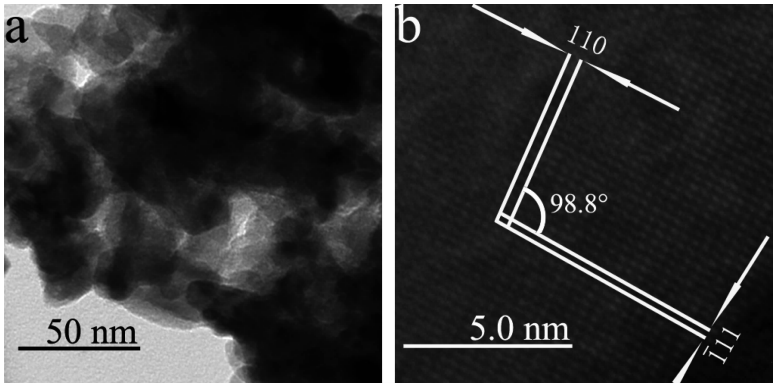

Fig.2 (a) TEM image of the as-prepared $FeWO_4$ nanoflakes; (b) HR-TEM image from a typical $FeWO_4$ nanoflake

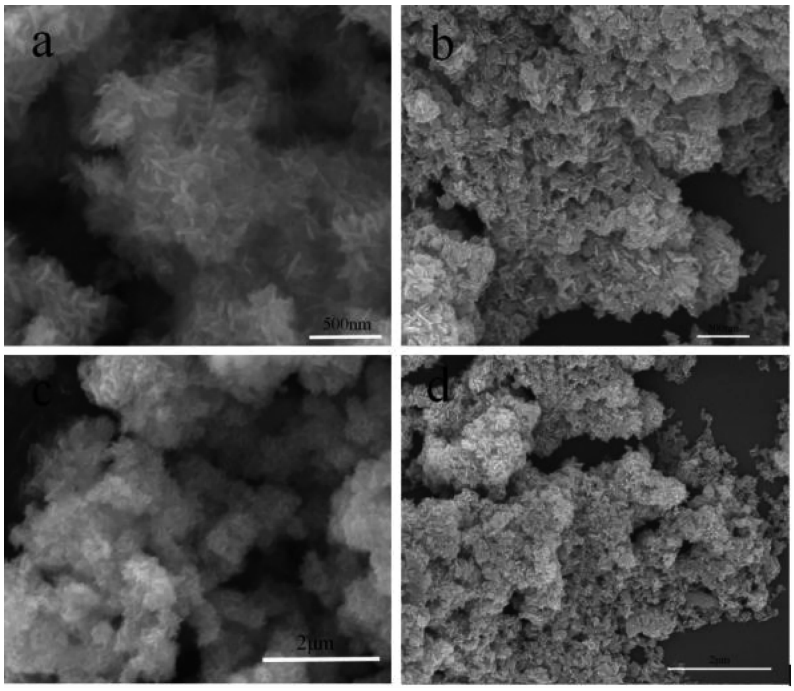

Fig.3 SEM images of unannealed (a, c) and annealed (b, d) $FeWO_4$ samples

The XPS spectrum of unannealed $FeWO_4$ microcrystals is shown in Fig.4. The main peak values at 34.0, 283.0, 529.0 and 711.0 eV, are labeled to the binding energies of W4*f*, C1*s*, O1*s*, and Fe2*p*, respectively. The strong intensity of C1*s* peak in Fig.4 intimates the abundance of carbonaceous adsorbents on the surface of the as-prepared $FeWO_4$ nanoparticles.

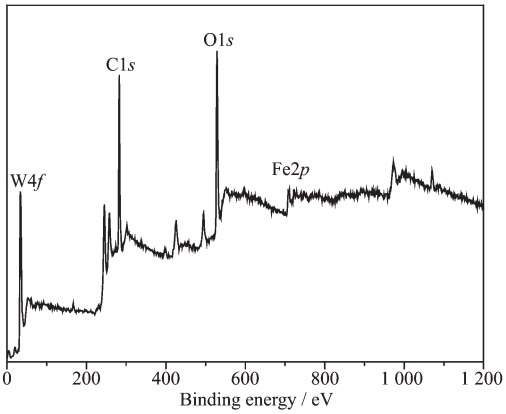

Fig.4　XPS spectrum of unannealed $FeWO_4$ samples

2.2　Photocatalytic activities

Employed as complexing agent, Na_2EDTA is crucial for the formation of $FeWO_4$ microcrystals, and plays an important role on the photocatalytic property. The degradation experiment of organic contaminants is performed. The RhB solution is chosen as a model reactant to demonstrate the impact of annealing treatment on photocatalytic property.

Fig.5 shows the UV-Vis absorption spectra during the photodegradation of RhB (initial concentration: 30 $\mu mol \cdot L^{-1}$, 30 mL) in the presence of 30 mg $FeWO_4$ sample under 500 W Xe lamp (modeling sunlight). Before the light on, to ensure the adsorption-desorption equilibrium completely, the suspensions were kept bubbling in darkness for 30 minutes. As shown in Fig.5(a), the absorption peaks at 556 nm belonging to RhB molecules gradually decreased as the reaction proceeding. The adsorption peaks at 556 nm completely disappeared only after 25 minutes, which reveal the excellent photocatalytic property of the $FeWO_4$ sample after annealing. $FeWO_4$ without any annealing treatment was also employed as photocatalyst. The result of the RhB degradation of samples is shown in Fig.5 (b). When the reacting time is set at 25 min, the value of C/C_0 is about 60%. Then, the degradation experiment by employing unannealed $FeWO_4$ was carried as long as enough (about 2 hours) until the absorbance values unchanged basically and the degradation rate was found as 77% ultimately.

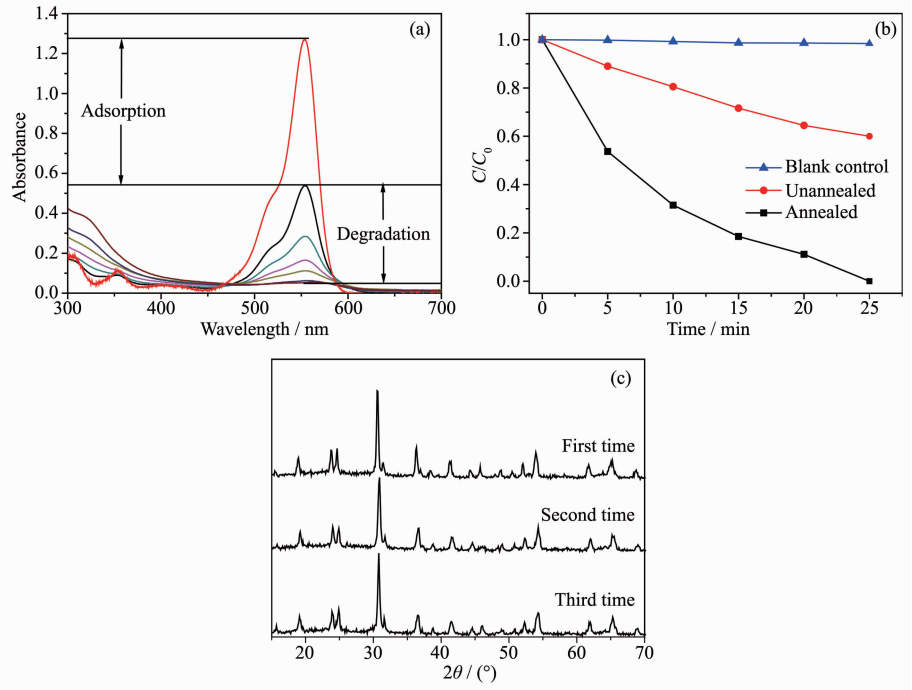

Fig.5　(a) UV-Vis absorbance spectra of the RhB solution in the presence of annealed $FeWO_4$; (b) Plots of C/C_0 vs time; (c) XRD patterns of $FeWO_4$ after three photocatalytic cycles

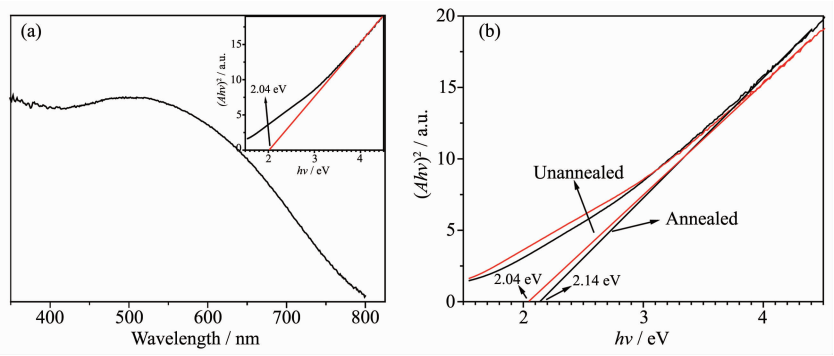

Fig.6 (a) UV-Vis diffuses reflectance spectra of the unannealed $FeWO_4$; (b) Contrast of E_g between the annealed and unannealed samples

The difference of photocatalytic properties of $FeWO_4$ samples before and after annealing is so apparent. For this degradation experiment, full adsorption played a key role in the first twenty minutes. In addition, three photocatalytic cycle experiments were carried out. RhB dyes were completely degraded, and the phase of $FeWO_4$ crystallite did not change according to XRD patterns in Fig.5(c).

The UV-Vis diffuses reflectance spectra of the $FeWO_4$ before and after annealing are shown in Fig.6 (a). There is a higher absorption range between 400 and 600 nm, implying the possibility of high photocatalytic activity of the samples under the visible light irradiation. The band gap of the as-prepared $FeWO_4$ was calculated via the equation[13]:

$$A h\nu=(h\nu-E_g)^n$$

A is the absorbance, h is the Planck constant, ν is the photon frequency, E_g is the energy gap, and n is the pure numbers associated with the different types of electronic transitions. The value of n for $FeWO_4$ equals to 1/2 and its band gap is estimated to be 2.04 eV, which has the same value to the reported values (*ca.* 2.0 eV) of bulk crystals[14]. The E_g values of the annealed and unannealed samples are displayed in Fig.6(b). E_g of the annealed is a little greater, possibly caused by the quantum size effect of the nanoparticles. These E_g values (2.04 and 2.14 eV) indicate that the $FeWO_4$ has a suited band gap for photocatalytic decomposition of organic pollutants under visible light irradiation.

TG analysis was performed in the atmosphere of air. As shown in Fig.7, there is only little of weight loss at 310 ℃, less than 2.0%, owing to the organic adsorbent burned to CO_2, H_2O or other residue in air. The weight loss arises 6.75% at 500 ℃, and eventually runs up to 8.05% from about 550 to 800 ℃. The latter indicates the possible transformation of $FeWO_4$ into other phases[15]. Therefore, the annealing treatment was set at 310 ℃, rather than higher temperature. In fact, the experiment with higher annealing temperature was performed for comparison. The product is better crystalline, probably ascribed to other phase, and poor in photocatalytic degradation experiment of RhB solution.

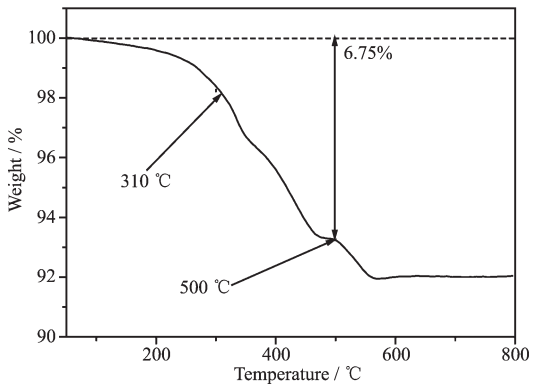

Fig.7 TG curve of as-prepared $FeWO_4$

Nitrogen adsorption-desorption isotherms of annealed $FeWO_4$ are shown in Fig.8. In the region of P/P_0=0~0.8, the adsorption isotherm and the desorption isotherm coincide into one line, indicating that there are not mesoporous structures in the $FeWO_4$ nanoflakes, and the region of P/P_0=0.8~1.0 indicates that accumulation holes exist between material particles. The specific surface area of as-prepared $FeWO_4$ samples is about 17 $m^2 \cdot g^{-1}$ and becomes about 11 $m^2 \cdot g^{-1}$ after

the annealing treatment, which is some different from expectation that the annealing treatment made the specific surface area not raised but decreased. During annealing process $FeWO_4$ nanoparticles might agglomerate and grow into larger crystals, which made specific area decreased[16]. It is reasonable to conclude that the specific surface area of $FeWO_4$ is not the decisive factor for its photocatalytic activity in RhB solution. The recombination of the photo-generated electrons and holes in the $FeWO_4$ microcrystals affected phtocatalytic activity in system. It can also be observed from the SEM images in Fig.3 that the grain size of $FeWO_4$ nanoparticles increased because of the gradual formation of larger crystals and the consequent coalescing.

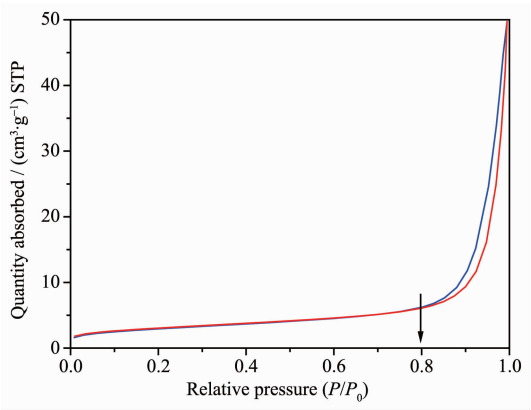

Fig.8　Nitrogen adsorption-desorption isotherms of $FeWO_4$ after annealing treatment

Besides, the organic residue was burned up during the annealing process, and the crystal faces, covered by the organic residue, were then exposed. The IR spectrum of the samples is shown in Fig.9, and the typical peaks of $FeWO_4$ are labeled in lines. Several peaks (773, 860 and 949 cm^{-1}) existing below 1 000 cm^{-1} and the broad band between 3 300 and 3 600 cm^{-1} are in consistence with the O-W-O stretching modes of WO_4^{2-}, respectively. The peaks below 700 cm^{-1} (including 509 and 657 cm^{-1}) are in consistence with the metal-oxygen (Fe-O) stretching vibrational mode. This result is in accord with the previous report[17]. In Fig.9(b), the peak at 1 468 cm^{-1} is labeled with the C-H in-plane bending vibration, and peaks at 2 850 and 2 922 cm^{-1} are labeled with C-H (saturated hydrocarbon) stretching vibration, indicating the presence of organic residue sticking to products, which accords with the XPS result in Fig.4. As shown in Fig.9(b), all peaks belonging to hydrocarbon bonds disappear, confirming that the organic residue could be eliminated by annealing treatment without destroying the initial nanostructure. The organic residue was transformed into carbon nanoparticle, enhancing the absorption of RhB, which is helpful to photodegradation of RhB. In conclusion, the introduction of complexing agent and then conversion into carbon nanoparticle are crucial in the reaction system, and Na_2EDTA plays an important role on the photocatalytic property.

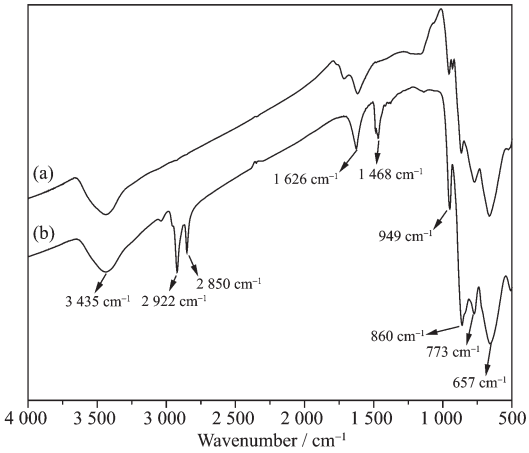

Fig.9　IR spectra of the annealed (a) and unannealed (b) samples

3　Conclusions

In summary, $FeWO_4$ microcrystals were fabricated through a simple solution-based method with Na_2EDTA and CTAB employed as complexing agent and surfactant, respectively. The photocatalytic property of $FeWO_4$ microcrystals on organic pollutant (RhB) were studied. $FeWO_4$ sample, being annealed under the circumstance of air with the temperature of 310 ℃ in the muffle furnace, shows highly active in degradation of RhB experiment. RhB solution with the concentration of 30 $\mu mol \cdot L^{-1}$ discolored only after 25 min under UV and visible light illumination, which was not reported before. The reason was probably relevant to the burning and carbonization of organic residue bound on $FeWO_4$ nanoparticles. This unique

$FeWO_4$ microcrystal is p otential for application in decontamination field, and the annealing method can be applied in other similar materials to improve their absorption and photocatalytic properties.

Acknowledgments: This work was supported by the Natural Science Foundation of Anhui Province (Grant No.1508085QB46).

References:

[1] (a)Chatterjee D, Dasgupta S. *J. Photochem. Photobiol. C*, **2005**, **6**(2/3):186-205
(b)Tong H, Ouyang S X, Bi Y P, et al. *Adv. Mater.*, **2012**,**24**(2):229-251
(c)LI Yao-Wu(李耀武), HUANG Chen-Xi(黄辰曦), TAO Wei(陶伟), et al. *Chinese J. Inorg. Chem.*(无机化学学报), **2017**,**33**(3):361-376
(d)Wang W N, Zhang F, Zhang C L, et al. *Chin. J. Catal.*, **2017**,**38**:1851-1859

[2] (a)Xu P, Zeng G M, Huang D L, et al. *Sci. Total Environ.*, **2012**,**424**(4):1-10
(b)Mishra M, Chun D-M. *Appl. Catal. A*, **2015**,**498**:126-141

[3] (a)Tan C Q, Xu C, Ren H J, et al. *J. Nano Res.*, **2017**,**46**:123-134
(b)Zhao Y, Yao K, Cai Q, et al. *CrystEngComm*, **2013**,**16**(2):270-276

[4] (a)Li D, Xue J, Liu M. *New J. Chem.*, **2015**,**39**(3):1910-1915
(b)Zhang L, Cao X F, Ma Y L. *New J. Chem.*, **2010**,**34**(9):2027-2033

[5] (a)Li L L, Peng S J, Wang N, et al. *Small*, **2015**,**11**(20):2429-2436
(b)YANG Ming-Rong(杨明荣), SHEN Yong(沈勇), HU Xiao-Sai(胡小赛), et al. *Chinese J. Inorg. Chem.*(无机化学学报), **2017**,**33**(7):1223-1230
(c)WANG Ling(王玲), WEN Wen(文雯), LI Sha(李莎), et al. *Chinese J. Inorg. Chem.*(无机化学学报), **2016**,**32**(3):393-404

[6] (a)Yao J, Yan H, Lieber C M. *Nat. Nanotechnol.*, **2016**,**8**(5):329-335
(b)Zhou H Y, Xiong S L, Wei L Z, et al. *Cryst. Growth Des.*, **2009**,**9**(9):3862-3867
(c)Huang M, Mi K, Zhang J H, et al. *J. Mater. Chem. A*, **2016**,**5**(1):266-274
(d)Zhang J H, Huang M, Xi B J, et al. *Adv. Energy Mater.*, **2017**,**8**(2):1701330

[7] (a)Shim H W, Cho I S, Hong K S, et al. *Nanotechnology*, **2010**,**21**(46):465602
(b)He G L, Chen M J, Liu Y Q, et al. *Appl. Surf. Sci.*, **2015**, **351**:474-479
(c)Hu W, Zhao Y, Liu Z, et al. *Chem. Mater.*, **2008**,**20**(17):5657-5665

[8] Kang S, Li Y Y, Wu M M, et al. *Int. J. Hydrogen Energy*, **2014**,**39**(28):16081-16087

[9] Zhou Y X, Yao H B, Zhang Q, et al. *Inorg. Chem.*, **2009**,**48**(3):1082-1090

[10]Guo J, Zhou X, Lu Y, et al. *J. Solid State Chem.*, **2012**,**196**:550-556

[11]Chen Z, Ma H, Xia J, et al. *Ceram. Int.*, **2016**,**42**(7):8997-9003

[12](a)Han Z, Ma Y, Guo Y, et al. *J. Solid State Chem.*, **2015**,**39**(7):5612-5620
(b)Zhang J, Wang Y, Li S K, et al. *CrystEngComm*, **2011**,**13**:5744-5750

[13]SHI Yong(石勇), JIN Zheng-Guo(靳正国), LI Chun-Yan(李春艳), et al. *Chinese J. Inorg. Chem.*(无机化学学报), **2005**, **21**(9):1286-1290

[14]Zhang J, Zhang Y, Yan J Y, et al. *J. Nanopart. Res.*, **2012**, **14**(4):1-10

[15]Sriraman A K, Tyagi A K. *Thermochim. Acta*, **2003**,**406**(1/2):29-33

[16](a)Nadzirah S, Hashim U, Kashif M, et al. *Microsyst. Technol.*, **2017**,**23**(6):1743-1750
(b)Xin G, Guo W, Ma T. *Appl. Surf. Sci.*, **2009**,**256**(1):165-169

[17]Zorina M L, Syritso L F. *J. Appl. Spectrosc.*, **1972**,**16**(6):774-776